International RILEM Conference on Materials, Systems and Structures in Civil Engineering
Conference segment on Concrete with Supplementary Cementitious Materials
22-24 August 2016, Technical University of Denmark, Lyngby, Denmark

PARTICLE SIZE DISTRIBUTION AND SPECIFIC SURFACE AREA OF SCM'S COMPARED THROUGH EXPERIMENTAL TECHNIQUES

Natalia M. Alderete[1,2], Yury A. Villagrán Zaccardi[2], Gabriela S. Coelho Dos Santos[2], Nele De Belie[1]

(1) Magnel Laboratory for Concrete Research, Department of Structural Engineering, Faculty of Engineering and Architecture, Ghent University, Belgium
(2) LEMIT Laboratory for Multidisciplinary Training in Technological Research, La Plata, Argentina

Abstract
Supplementary cementitious materials (SCMs) are mainly used to produce a green concrete. To reach that goal effectively, it is highly important to adequately characterize the SCMs. It is well known that particle size distribution (PSD) and fineness of SCMs have a great influence on concrete properties. Traditionally, cement fineness has been assessed by the specific surface area (SSA) through the Blaine method (BM). However, the BM has the simplification of considering ideal spherical shape particles. The BET theory has also been used to calculate SSA, however, also some assumptions may lead to inaccuracy in the calculations. Both PSD and SSA can be evaluated through Laser Diffractometry (LD), but this technique also considers ideal spherical particles as a simplification. Regardless of the mentioned drawbacks, these techniques provide useful information to characterize SCMs provided that the limitations are considered. In this paper, Ground Granulated Blast Furnace Slag (GGBFS), Natural Pozzolan (NP) and Limestone Powder (LP) are tested using the BM, LD, and nitrogen adsorption. Particle texture and shape are assessed through petrography and scanning electron microscope (SEM). Results from BM, BET and LD are compared, analysing the possible effects of particle shape and texture.

1. Introduction

Fineness from supplementary cementitious materials (SCMs) is generally evaluated as an influencing parameter on the properties of concrete. However, the assessment of fineness through different experimental techniques is not usually considered adequately, and some limitations are disregarded leading to an incorrect interpretation of results. Generally, standard methods used to assess physical properties of cement have been straightforwardly applied for SCMs without any modification. However, the same techniques may not always be applicable due to differences in shape and size of SCMs.

For the determination of the specific surface area (SSA), the Blaine method (BM) has been commonly used for cement [1- 3]. BM is a rather empirical method particularly designed for cements, and therefore its application for SCMs requires some adaptations. For example, a different plunger has been proposed by [4] to avoid removing it. This modified plunger was used by [5] to test silica fume with unsatisfactory results as a well compacted bed could not be achieved.

Alternatively to the BM, laser difractometry (LD) is a quick technique that uses the optical properties of the powder to evaluate both its SSA and its particle size distribution (PSD). LD has been fairly well described in [6-8], where the importance of the dispersion conditioning and the correct selection of the optical parameters are highlighted. Another technique for SSA determination is the use of the Brunauer, Emmett, and Teller (BET) theory [9] which is based on the amount of gas adsorbed on a monomolecular layer on the surface. This has the evident advantage of not assuming a specific particle shape; however, some simplified assumptions, as the existence of a homogenous covering layer [10] may not lead to the actual SSA value.
In this study, fineness of Ground Granulated Blast Furnace Slag (GGBFS), Natural Pozzolan (NP) and Limestone Powder (LP) is measured and compared with the three techniques. Guidelines in ASTM C204-07 [11] for the application of the Blaine method to materials other than cement are followed. Some recommendations in addition to those in the literature are proposed to obtain reliable results from LD. Finally, the results are compared with characterization through petrography and scanning electron microscopy (SEM), with assessment of particle shape and texture and their influence on the values obtained and the theoretical considerations of each method.

2. Materials and methods

2.1. Materials

This study includes analysis of ground granulated blast furnace slag (GGBFS), natural pozzolan from volcanic origin (NP) and limestone powder (LP). Both GGBFS and NP were first dried in oven for 24 h, and then ground in a laboratory ball mill for cement, with the aid of cylpebs. The grinding process was carried out for 1.5 h for the GGBFS and 2.0 h for the NP. LP was also processed in an industrial ball mill. The chemical composition of the materials is shown in Table 1.The chemical analysis was performed by X-ray fluorescence and the density was determined according to ASTM C188-15 [12].

Table 1: Chemical compositions of GGBFS, NP and LP.

wt (%)	**GGBFS**	**NP**	**LP**
CaO	36.16	1.34	48.85
SiO_2	28.89	62.53	8.15
MgO	12.14	1.13	1.41
Al_2O_3	8.62	10.76	1.28
Na_2O	1.91	5.66	1.25
SO_3	1.85	0.34	0.05
Fe_2O_3	0.95	1.81	0.88
TiO_2	0.46	0.09	-
K_2O	0.43	3.67	0.28
MnO	0.43	0.06	0.04
LOI	nd-	nd-	37.29
Density (g/cm^3)	2.92	2.41	2.71

nd = not determined

2.2. Methods

2.2.1. Blaine method

The BM test was performed according to ASTM C204-07 [11], where the special consideration for materials other than cement intends to consider the possible differences in density, porosity or shape in relation to a standard reference material.

2.2.2. Laser diffraction

The particle size distribution by means of LD was determined using a particle analyser Malvern Mastersizer 2000 E, wet unit Hydro 2000SM (A). Isopropanol (IPA) was used as a dispersant for the three SCMs. For the refractive index (m = n+ ik), different values of refraction index (n) and absorption coefficient (k) were used for each SCM, according to the data found in literature [6-8]. Those combinations of values which had the best fit and less weight residual were selected. Selected values of n and k are presented in Table 2.

As described in [6] duration of dispersion, ultrasonication frequency, stirrer rate, measurement time and obscuration levels were first optimized in order to obtain reliable results for each of the SCMs. Particular attention was paid to the dispersion procedure since failure in this step leads directly to erroneous results. The selected procedure consisted of 5 minutes of ultrasonic bath (35 kHz, 320 W), 1700 rpm for the stirrer rate, 20 s of measuring time and 11.5 ± 0.5% of obscuration level. After the de-agglomeration of the particles was finished, a syringe was used to collect the sample and place it inside the diffractometer. The same procedure (stirring speed, sonification time and frequency, sample and background measurement time, obscuration level) was applied for all the SCMs changing only the values of n and k for each particular case.

Table 2: Selected optical parameters of the SCMs.

	GGBFS	NP	LP
n	1.62	1.49	1.57
k	0.1	0.1	0.05

2.2.3. BET method

For quantitative analysis, adsorption and desorption curves using nitrogen at 77 K were determined with a Micromeritics Asap 2020. Before measurement, samples were dried at 105°C and kept in a desiccator until testing. The BET adsorption theory was used for the determination of surface area, using the corresponding values of the relative pressure between 5-35% of the adsorption curve.

2.2.4. Petrographic characterization

2.2.4.1 Petrographic microscope

Petrographic characterization of the SCMs was done in accordance to ASTM C295 [13]. The equipment used is an Olympus BH2-UMA petrographic microscope. This instrument includes an Infinity 1-3C digital camera of13.1 megapixels. Image processing was done with Infinity Analyze 5.0 software.

2.2.4.2 Scanning electron microscope (SEM)

The SEM allows analysing materials morphology with micrometric detail. All the information registered can be translated into external morphology and materials orientation [14]. A SEM 505 Philips was used to perform the characterization.

3. Results

3.1. Blaine method

Some difficulties for achieving an adequate bed height with a given porosity (ε) have been found when testing SCMs [5]. The ASTM C204-07 addresses this problem by calculating a constant (b) appropriate for each sample, which is obtained by plotting the values of $\sqrt{(\varepsilon^3.T)}$ versus ε and determining the y-intercept by linear regression. For the calculation of the value of b, a minimum of 12 determinations have to be made.

Four samples of each SCM were tested at four different ε values, and the b characteristic value of each SCM was calculated. The results of the SSA and the bed porosity range used for each material are shown in Table 3.

Table 3: Blaine SSA and bed porosity range of the SCMs

	GGBFS	NP	LP
Porosity values	0.53,0.55,0.57,0.59	0.53,0.55,0.57,0.59	0.47,0.49,0.51,0.53
Surface area (m^2/kg)	341±4	858±12	646±5

3.2. Laser diffraction

It has been pointed out by several authors [5, 7, 8] that the chosen refractive index has a great influence on the results of PSD measured by LD. This is directly related to the basic principle of laser diffractometry given that scattering arises when there are differences in the refractive index of the particle and the surrounding medium [15]. If there is no information available about the optical properties of the sample, generally different combinations of n and k are tested, and then the most appropriate combination is chosen from the results obtained. The weight residual indicates how well the optical model of Mie fits the registered scattering pattern, and it is defined as the % error between the data measured and data corrected with parameters [16]. In order to keep a standard criterion, the weight residual of each measurement was compared in this study. The lowest value obtained for the different values of m used was considered the most reliable combination. LP measurements had the lowest mean weight residual and NP had the highest weight residual value. Figure 1 shows the PSD of triplicate measurements for each SCMs. Table 4 shows the values of surface area, dv10, dv50 and dv90 for each SCMs, using the described procedure and the optical parameters indicated in Table 2. The calculations of the surface area were made under the assumption of spherical particles.

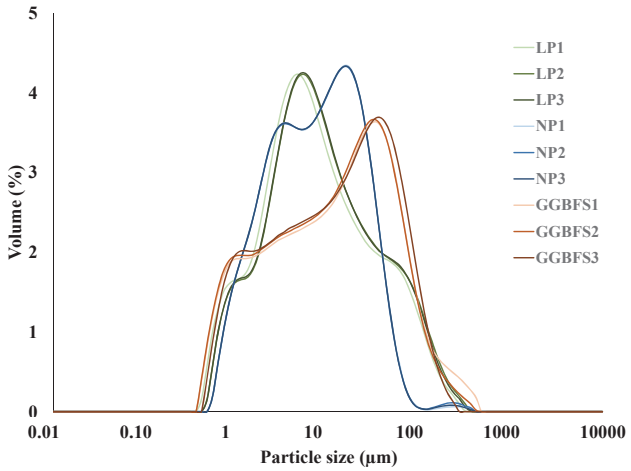

Figure 1: Particle size distribution of LP, NP and GGBFS

Table 4: PSD of the SCMs

	GGBFS	NP	LP
dv10 (µm)	1.14± 0.03	1.36±0.001	1.27 ± 0.12
dv50 (µm)	12.73 ± 0.67	7.05± 0.02	7.67 ± 0.63
dv90 (µm)	66.27 ± 7.18	28.14± 0.16	72.88 ± 10.4
Surface area (m^2/kg)	566 ± 13	701±2	606 ± 13

3.3. BET method

Values obtained from the adsorption and desorption nitrogen curve are shown in Figure 2. With the BET theory, the SSA accessible to nitrogen molecules were calculated within the low RH range of the adsorption isotherms. The results obtained were 987.3m^2/kg, 2255.7m^2/kg and 3900.4m^2/kg for GGBFS, NP and LP respectively.

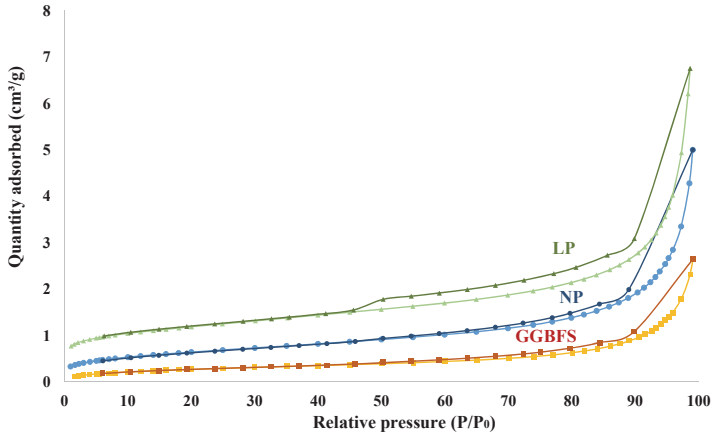

Figure 2: Sorption and desorption curves from Nitrogen gas of LP, NP and GGBFS

3.4. Petrographic characterization

3.4.1. Petrographic microscope

Figure 3 shows two petrographic images with 100x and 200x magnification for GBFFS (A.1 and A.2), LP (B.1and B.2), and NP (C.1and C.2). Their description is as follows.

3.4.1.1. GGBFS

The material is mainly composed of irregular and/or plank-shaped particles, which have a sharp or hook-shaped end (A.1, A.2). All particles are transparent with high relief. With crossed polars they are mostly isotropic, showing their amorphous character. Though, there are some anisotropic grains with high birefringence, which belong to crystalline particles of tabular development, possibly melilite. Particle size is estimated to be in the range 10-75 µm.

3.4.1.2. LP
Under polarized light transparent or grey/yellow particles can be seen (B.1, B.2). Their shape is mainly sub-rounded, some smaller than 5 μm, and some particles have a maximum size of 10 μm. Due to their small size; these particles have a tendency to agglomerate, forming aggregates up to 100 μm, although these agglomerations are rare. Under crossed polars LP particles show a high interference color, similar to yellow, and typical of calcite.

3.4.1.3. NP
NP sample is mainly composed of vitreous transparent particles, of low relief, irregular morphology and conchoids and sharp edges typical of this kind of materials (C.1, C.2). Their size range is mainly between 2-20 μm. Some minor large (60-100 μm) brown sheet-like particles, corresponding to biotite are also present. All these petrographic characteristic are typical of a glassy material from volcanic origin.

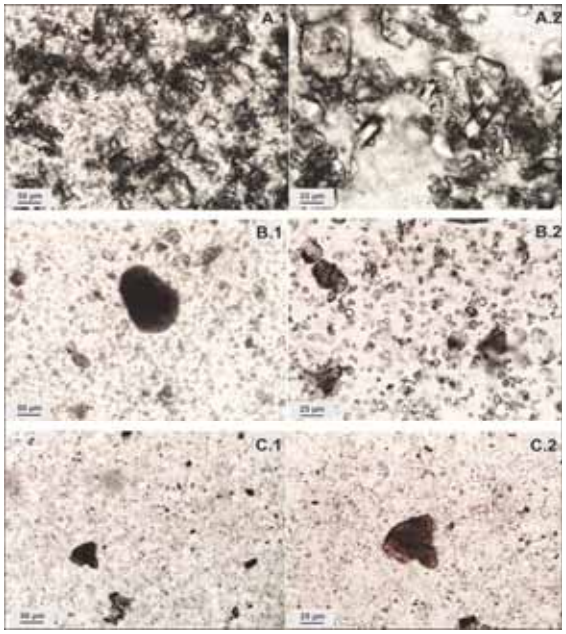

Figure 3: Petrographic microphotographs with parallel light with 100x and 200x of magnification of GGBFS (A1,A2), LP (B.1, B.2) and NP (C.1,C.2), respectively

3.4.2.SEM characterization
Figure 4 shows two SEM images for GBFFS (A.1 and A.2), LP (B.1, and B.2), and NP (C.1 and C.2). Their description is as follows.

3.4.2.1. GGBFS
A wide variation in the grain size can be seen for the GGBFS samples in A.1 and A.2. Individual particles are angular or sub-angular and have a smooth surface, in some particles micrometric pores can be seen with spherical morphology. This could be attributed to the fast

cooling of the particles when they formed. A detailed picture of this is shown in A.2., where a 50µm particle can be seen filled with smaller GGBFS particles.

3.4.2.2. LP
From B.1 and B.2 images, high content of fine particles of the material can be seen, especially in the range of 0.1-5 µm, but with some minor content of large particles (50-100 µm) sometimes as a product of agglomeration of smaller particles. Most of the particles are sub-rounded and smaller particles can be seen adhered in their surface.

3.4.2.3. NP
Particle size range of NP is generally around 50 µm or lower, as seen in C.1 and C.2. NP particle shape is mostly angular or sub-angular, of conchoidal fracture, with sharp edges - typical for vitreous materials-and smooth surface. Some smaller particles can be seen adhered as well.

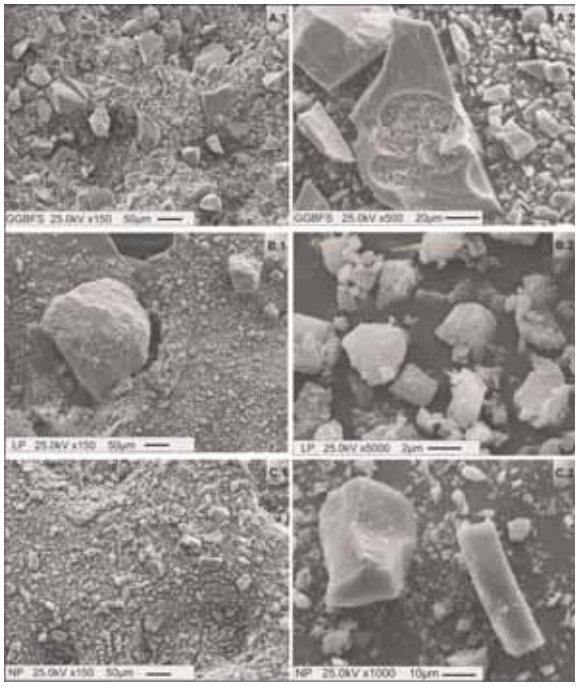

Figure 4: SEM micrographs of GGBFS (A.1, A.2),LP(B.1, B.2), and NP(C.1, C.2).

4. Discussion

Figure 5 presents a comparison between the SSA obtained with BM, LD and BET, where a clear discrepancy among the different techniques can be seen. In the case of the BM, low standard deviations were found for the SSA calculation considering the characteristic b value for each sample. According to the results, NP is the finest SCM, followed by LP and GGBFS.

This seems to be in disagreement with the petrographic and SEM observations, where LP seems to have the smallest particle size. There is a wider particle size range for LP, resulting in a lower specific surface in spite of the high number of fine particles. This is due to the prevalence of large and heavy particles over the high surface area of small particles. Although is very difficult to make this objective evaluation by simple observation. Calculations of the span of the distribution were made as the difference between dv90 and dv10, divided dv50. The results for GGBFS, LP, NP and were 5.12, 9.34, 3.80, and respectively. This parameter is a measurement of the width of the distribution, where LP has the broadest PSD.

The value of the median size, $\overline{x}$, and the uniformity factor, n, were calculated from the Rosin, Rammler, Sperling and Bennett (RRSB) distribution, graphical linearization was based on the 0.5-80% part of the PSD. The results from triplicate measurements of $\overline{x}$ are 20.49, 12.30 and 10.18 μm for GGBFS, LP and NP respectively. The results of n are 0.75, 0.97, and 1.06 for GGBFS, LP and NP respectively. There is a clear distinction in the highest value of the median particle size, for GGBFS in relation to the other, which indicates its coarser PSD.

Also, part of this difference could be attributed to the particles shape and packing of the sample bed, since the air flow around a rounded particle (which is the case of LP) would be faster than through semi-angular particles, as is the case for NP particles. Furthermore, the compaction of the sample bed may not be the same for different particle shapes and hence results would not be totally comparable. In fact, it has been suggested [6] that there is no possible comparison if the reference material does not have similar shape, particle size distribution, and surface properties to the material of interest. Then, in spite that the method proposed by the standard [11] intends to account for these differences, the practical approach still does not provide completely reliable results. Even some authors [17], completely disregard the method for considering it an indirect and too simplified method.

With regards to the LD technique, NP seems to be the finest SCM, followed by LP and GGBFS. The high value obtained for NP could be explained by the particle shape of the sample, which is mostly angular or sub-angular, of conchoidal fracture and sharp edges. These characteristics significantly differ from the assumption of spherical particles for the computation of SSA from LD results. This simplification also causes the largest weight residual values for NP among the three materials. The fact that GGBFS and LP have similar SSA values for LD but not for BM also shows the influence of the particle shape. It seems that particle shape does not allow the same compaction factor for BM, but the influence is not so significant for LD, as the particle size distribution is not so different. Furthermore, rounded LP particles have a better fit to the hypothesis for the calculations (also represented in the lower weight residual value obtained for LP) while GGBFS SSA is influenced by the angle in which its semi-angular or planked-shaped particles would pass through the incident laser beam.

From BET results, LP has the larger SSA, followed by NP and GGBFS. From XRD with Rietveld analysis, a composition of 75% calcite and 10% quartz was determined for LP. Clay impurities could not be detected, but it would still be possible that this is the cause for such a high SSA from BET calculations. These calculations assume a monolayer covering the area of each particle and then particle shape is automatically taken in consideration and has been

considered a good representative technique of the SSA [18]. Yet, it is not possible to verify that always a continuous and perfectly uniform monolayer is achieved. Besides, the size of the adsorbate can modify the BET results [10]. It can also be seen that BET SSA values are always larger than those from BM and LD, for all SCMs. This has also been mentioned before by [5], and it is attributed to the fact that gas molecules access cracks and pores of the particles. In this sense, nitrogen adsorption is not much affected by aggregation of particles, which was mostly observed for LP, and whereas this aggregation results in lower SSA computed from BM or LD (as they assume an aggregate as an individual spherical particle), nitrogen is able to penetrate spaces between particles in these aggregates and the SSA computed on this basis is higher. From the comparison, it is derived that SSA values computed from BM and LD are reduced because in this case the inner porosity is not considered and in the case of LP also by aggregation of particles.

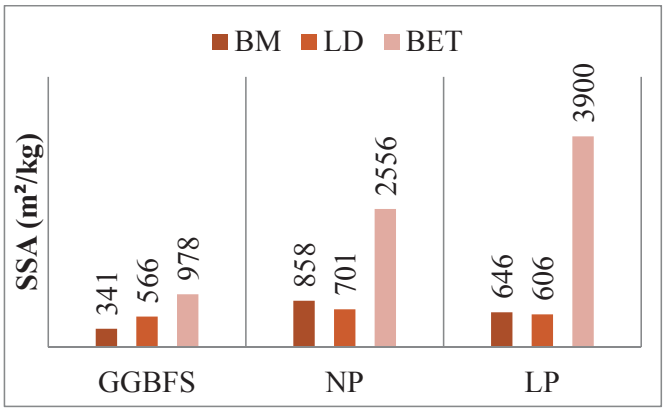

Figure 5: Comparison among BM, LD and BET surface area results for each SCMs.

5. Conclusions

Results from different commonly used techniques have been presented for the evaluation of the particle size and SSA of GGBFS, NP and LP.

Particle shape showed significant influence on the results obtained. This is specially seen for SSA calculations with BM and LD since the assumptions of spherical particles can greatly influence the results. Particularly the BM does not show reliable results, given that it cannot effectively evaluate the SSA for comparative purposes if the particle shape interferes in the bed compaction. On the other hand, LD for particle size distribution seems to be a consistent method in order to obtain reliable results regarding PSD, but SSA computed on this basis may be inaccurate. Furthermore, it is highly recommendable to achieve good particle dispersion and to evaluate different refraction index and absorption coefficient combinations and select the one with the lowest weight residual value. In the case of the BET SSA calculations, results were found to be in agreement with the characterization by microscopy. Moreover, increased

values for the SSA were obtained from nitrogen adsorption in correspondence with the consideration of inner porosity and the limited influence of particle aggregation on the results. Each technique has its own limitations, and each SCMs its own characteristics, therefore absolute values should be carefully considered, and keeping in mind the limitations.

References

[1] Hu J., Ge Z., Wang K. Influence of cement fineness and water-to-cement ratio on mortar early-age heat of hydration and set times. Construction and Building Materials 50 (2014), pp 657–663
[2] Celik I.B., Oner M., Can N. M. The influence of grinding technique on the liberation of clinkerminerals and cement properties. Cement and Concrete Research 37 (2007), pp 1334–1340
[3] Celik I.B. The effects of particle size distribution and surface area upon cement strength development. Powder Technology 188 (2009), pp 272–276
[4] Teipel U, Winter H Characterization of the specific surface area with the permeation method. In: At mineral processing 52(2011)
[5] Arvaniti E. C, Juenger M. C. G., BernalS. A., Susan A., Duchesn J., Courard L., Leroy S., Provis J. L., Klemm A., De Belie N. Determination of particle size, surface area, and shapeof supplementary cementitious materials by different techniques. Materials and Structures, (2014), DOI 10.1617/s11527-014-0431-3
[6] Arvaniti E. C, Juenger M. C. G., BernalS. A., Susan A., Duchesn J., Courard L., Leroy S., Provis J. L., Klemm A., De Belie N. Physical characterization methods for supplementary cementitious materials. Materials and Structures (2015) 48:3675–3686
[7] Ferraris C. F., Bullard J. W., Hackley V. Particle size distribution by LASER diffraction spectrometry: application to cementitious powders. National Institute of Standard and Technology. 100 Bureau Drive. Gaithersburg MD 20899
[8] Cyr M, Tagnit-Hamou A. Particle size distribution of fine powders by LASER diffraction spectrometry. Case of cementitious materials. Materials and Structures, Vol. 34, (2001), pp 342-350
[9] Barret E., Joyner L., Halenda P., (1951). The determination of pore volume and area distributions in porous substances - computations from nitrogen isotherms, J. Am. Chem. Soc. 73, pp 373-380
[10] Stadie, Nicholas P. (2013) Synthesis and thermodynamic studies of physisorptive energy storage materials. Dissertation (Ph.D.), California Institute of Technology
[11] ASTM C204, Standard test method for fineness of hydraulic cement by air-permeability apparatus, American Society for Testing and Materials, USA (2007)
[12] ASTM C188, Standard test method for density of hydraulic cement, American Society for Testing and Materials, USA (2015)
[13] ASTM C295, Standard Guide for Petrographic Examination of Aggregates for Concrete, American Society for Testing and Materials, USA (2008)
[14] John D. A., Poole A. B., Sims I., John D. A., Concrete petrography, Published by CRC Press, (1998)

[15] Ma Z., Merkus H.G., Smet J., Heffels C., Scarlett B. New developments in particle characterization by laser diffraction: size and shape Powder Technology 111 (2000), pp 66–78
[16] Webb P. J. A Primer on Particle Sizing by Static Laser Light Scattering. Technical Workshop Series: Introduction to the Latest ANSI/ISO Standard for Laser Particle Size Analysis (2000)
[17] CepuritisR.,Wigum B.J., Garboczi E.J. , Mørtsell E. Jacobsen S. Filler from crushed aggregate for concrete: Pore structure, specific surface, particle shape and size distribution. Cement & Concrete Composites 54 (2014), pp 2–16
[18] Fagerlund G. Determination of specific surface by the BET method. Mater Struct, 6 (3) (1968), pp. 239–245